Cbfβ2 deficiency preserves Langerhans cell precursors by lack of selective TGFβ receptor signaling

Mari Tenno,[1] Katsuyuki Shiroguchi,[2,3,5] Sawako Muroi,[1] Eiryo Kawakami,[4] Keita Koseki,[4] Kirill Kryukov,[6] Tadashi Imanishi,[6] Florent Ginhoux,[7] and Ichiro Taniuchi[1]

[1]Laboratory for Transcriptional Regulation and [2]Laboratory for Immunogenetics, RIKEN Center for Integrative Medical Sciences, Yokohama, Japan
[3]Laboratory for Integrative Omics, RIKEN Quantitative Biology Center, Osaka, Japan
[4]Disease Biology Group, RIKEN Medical Sciences Innovation Hub Program, Yokohama, Japan
[5]PRESTO, Japan Science and Technology Agency, Saitama, Japan
[6]Biomedical Informatics Laboratory, Department of Molecular Life Science, Tokai University School of Medicine, Kanagawa, Japan
[7]Singapore Immunology Network, Agency for Science, Technology, and Research, Singapore

The Journal of Experimental Medicine

The mouse Langerhans cell (LC) network is established through the differentiation of embryonic LC precursors. BMP7 and TGFβ1 initiate cellular signaling that is essential for inducing LC differentiation and preserving LCs in a quiescent state, respectively. Here we show that loss of Cbfβ2, one of two RNA splice variants of the *Cbfb* gene, results in long-term persistence of embryonic LC precursors after their developmental arrest at the transition into the EpCAM^{+} stage. This phenotype is caused by selective loss of BMP7-mediated signaling essential for LC differentiation, whereas TGFβR signaling is intact, maintaining cells in a quiescent state. Transgenic Cbfβ2 expression at the neonatal stage, but not at the adult stage, restored differentiation from Cbfβ2-deficient LC precursors. Loss of developmental potential in skin-residential precursor cells was accompanied by diminished BMP7–BMPR1A signaling. Collectively, our results reveal an essential requirement for the Cbfβ2 variant in LC differentiation and provide novel insight into how the establishment and homeostasis of the LC network is regulated.

INTRODUCTION

The skin is one of the body's largest interfaces and is exposed to the outer environment, functioning as a physical barrier to protect against the invasion of pathogenic microorganisms. In addition to mechanical defense, two immune populations, namely dendritic epidermal T cells (DETCs) and Langerhans cells (LCs), reside specifically in the epidermis and participate in immunosurveillance. LCs are skin-specific dendritic cells that play an essential role in sensing pathogenic microorganisms and tissue damage to initiate immune responses and maintain skin homeostasis (Merad et al., 2008; Chopin and Nutt, 2015; Hieronymus et al., 2015; Collin and Milne, 2016). Consistent with such functions, the LC network is established immediately after birth when animals become exposed to the outside environment. Previous studies in mice showed that LC precursors, which arise from both yolk sac and fetal liver precursors (Hoeffel et al., 2012), migrate to the epidermis at 16.5 to 18.5 d postcoitus (dpc; Romani et al., 2010) and undergo sequential differentiation during neonatal periods to generate the adult LC network (Ginhoux and Merad, 2010; Perdiguero and Geissmann, 2016). During differentiation into mature LCs, precursors exhibit altered morphology, such as the protrusion of dendrites, and express the C-type lectin Langerin, MHC class II, and epithelial cell adhesion molecule (EpCAM; Chorro et al., 2009). Simultaneously, a proliferative burst in LC precursors begins at approximately postnatal day (P) 3, resulting in the establishment of a primary LC network in the epidermis within a week after birth in mice (Chorro et al., 2009; Ginhoux and Merad, 2010).

Adult LC steady-state homeostasis is maintained throughout life without replenishment by circulating precursors (Merad et al., 2008), whereas conventional DCs, which reside in other tissues, are continuously replaced by cells that differentiate from BM-derived DC precursors (Merad et al., 2008; Ginhoux and Merad, 2010; Chopin and Nutt, 2015; Schlitzer et al., 2015; Collin and Milne, 2016). In contrast, when the LC network is impaired by genetic treatment, such as in inducible Langerin-DTR mice (Bennett et al., 2005; Nagao et al., 2009), or via artificial or natural inflammation (Ginhoux et al., 2006; Seré et al., 2012), BM-derived Gr-1^{+} monocytes migrate to the epidermis to replenish the LC network.

The importance of the TGFβ superfamily in LC network formation has been studied in depth in both humans and mice. These studies highlight the role of the TGFβ superfamily as a major soluble environmental cue required for establishing the primary LC network (Merad et al., 2008;

Correspondence to Ichiro Taniuchi: ichiro.taniuchi@riken.jp

Abbreviations used: 4-OHT, 4-hydroxytamoxifen; DETC, dendritic epidermal T cell; dpc, day postcoitus; EpCAM, epithelial cell adhesion molecule; LC, Langerhans cell; VDR, vitamin D receptor.

The Rockefeller University Press
J. Exp. Med. 2017 Vol. 214 No. 10 2933–2946
https://doi.org/10.1084/jem.20170729

Collin and Milne, 2016). TGFβ superfamily signaling is triggered by binding to heterodimeric receptors, composed of a variable type I receptor that has distinct affinity to each TGFβ superfamily member and one common type II (TGFβR2) receptor. TGFβR2 is essential for the initiation of the intracellular signaling cascade, which activates several signal transducers including SMAD family proteins (Chen and Ten Dijke, 2016; Collin and Milne, 2016). Mice with genetic ablation of TGFβ1 or TGFβR2 lack the LC network in the epidermis (Borkowski et al., 1996; Kaplan et al., 2007). These findings confirm that TGFβ1 controls LC differentiation. However, more recent studies revealed another unexpected function of TGFβ1 signaling in the control of LC homeostasis. Ablation of TGFβ1 or TGFβR1 in mature LCs enhanced their egress from the epidermis (Kel et al., 2010; Bobr et al., 2012). Thus, TGFβ1 signaling through TGFβR1 is essential to preserve LCs in a quiescent state in addition to mediating their differentiation (Collin and Milne, 2016). Moreover, a recent study proposed that another member of the TGFβ superfamily, BMP7, plays a more prominent role in LC differentiation via binding to BMP receptor 1A (BMPR1A; Yasmin et al., 2013a). Thus, the current model of LC differentiation and homeostasis proposes that BMP7 and TGFβ1 are involved in distinct pathways, with BMP7 controlling cellular signaling that induces LC differentiation and TGFβ1 preserving the quiescent state of LCs (Collin and Milne, 2016). However, it remains unclear how cellular signaling, triggered by related but distinct TGFβ superfamily members, is regulated to control distinct cellular functions.

Several transcription factors are essential for LC differentiation. Both Id2 and PU.1 were shown to be required for LC differentiation from embryonic precursors (Seré et al., 2012; Chopin et al., 2013). However, LC differentiation from BM precursors depends only on PU.1 and not on Id2 (Chopin et al., 2013). Runx3 is another transcription factor that is essential for LC development (Fainaru et al., 2004). Runx3 belongs to the Runx protein family, which functions by forming heterodimers with the non-DNA binding β-subunit, Cbfβ protein (Wang et al., 1996). In mammals, two RNA splice variants, Cbfβ1 and Cbfβ2, are generated from a single *Cbfb* gene, and each variant has distinct amino acid sequences at the C terminus (Ogawa et al., 1993). However, whether Cbfβ1 and Cbfβ2 have nonredundant functions, particularly in regard to LC differentiation and homeostasis, has not been clarified in animal models.

In this study, we unraveled the essential function of Cbfβ2 in driving LC differentiation from embryonic precursors. Despite the complete inhibition of LC differentiation, embryonic-derived LC precursors were still detectable in the adult epidermis of Cbfβ2-deficient mice. Mechanistically, we showed that this was caused by the selective impairment of TGFβR signaling, which is essential only for promoting LC differentiation. Rescuing Cbfβ2 expression, using a novel transgenic model, resulted in the resumption of LC differentiation only during the neonatal stage, and not at the adult stage. Such defects in the developmental potential of LC precursors at the adult stage were caused by the intrinsic loss of BMP7/BMPR1A signaling, an essential driver of LC differentiation.

RESULTS

Cbfβ2-deficient mice lack epidermal LCs

To address the unique functions of *Cbfb* splice variants, we generated a mouse model lacking either Cbfβ1 or Cbfβ2 expression. Based on flow cytometric analyses (Fig. 1 A) of epidermal sheets from 2-mo-old Cbfβ2-deficient mice (*Cbfb*$^{2m/2m}$), only a few cells expressed MHC-II, whereas expression in the epidermal sheet of Cbfβ1-deficient mice (*Cbfb*$^{1m/1m}$) was similar to that in wild-type (*Cbfb*$^{+/+}$) mice. Immunohistochemical analyses indicated that MHC-II$^+$ cells in the epidermis of *Cbfb*$^{2m/2m}$ mice lacked Langerin expression. In addition, CD3$^+$ DETCs, known as skin-specific γδT cells, were not present in the epidermis of *Cbfb*$^{2m/2m}$ animals (Fig. 1, A and B). Thus, as with Runx3-deficient mice (Fainaru et al., 2004), Cbfβ2 deficiency resulted in a lack of LCs and DETCs in the skin, although a few MHC-II$^+$ cells were present in the *Cbfb*$^{2m/2m}$ epidermis. These MHC-II$^+$ cells showed dendritic morphology, were larger than control *Cbfb*$^{+/+}$ MHC-II$^+$ LCs (Fig. 1 B), and expressed F4/80 and CD11b (Fig. 1 C), which are LC-lineage markers known to be expressed from an early developmental stage (Chorro et al., 2009). Importantly, these MHC-II$^+$ cells did not express mature LC markers (Fig. 1 C), such as CD11c, EpCAM, and CD24 (Chorro et al., 2009), but highly expressed the CX3 chemokine receptor 1 (CX3CR1; Fig. 1 D), a known marker expressed in recently seeded embryonic day (E) 18.5 LC precursors but not in differentiated LCs (Hoeffel et al., 2012). However, because these remaining MHC-II$^+$ CX3CR1-GFP$^+$ cells in the adult *Cbfb*$^{2m/2m}$ epidermis retained a marker signature reminiscent of LC precursors, we hypothesized that they represent LC precursors that are blocked in their differentiation, prompting us to next examine LC ontogeny in *Cbfb*$^{2m/2m}$ mice.

LCs developmentally arrest at approximately P3 in the *Cbfb*$^{2m/2m}$ epidermis

LC differentiation from embryonic precursors begins around birth (P0; Merad et al., 2008). As previously reported (Chorro et al., 2009), embryonic LC precursors at P0 can be defined as CD45$^+$CD3$^-$CD11b$^+$F4/80$^+$ cells. No significant difference in the percentage of epidermal cells was detected in *Cbfb*$^{2m/2m}$ newborns compared with *Cbfb*$^{+/+}$ controls (Fig. 2, A and B), indicating that in these cells, embryonic generation and skin-homing programs were unaffected by Cbfβ2 loss. Induction of MHC-II followed by EpCAM and Langerin expression concomitant with the loss of CX3CR1 expression represents normal LC differentiation after birth (Chorro et al., 2009; Nagao et al., 2009). At P0, 10–20% of CD45$^+$CD3$^-$CD11b$^+$F4/80$^+$ cells expressed

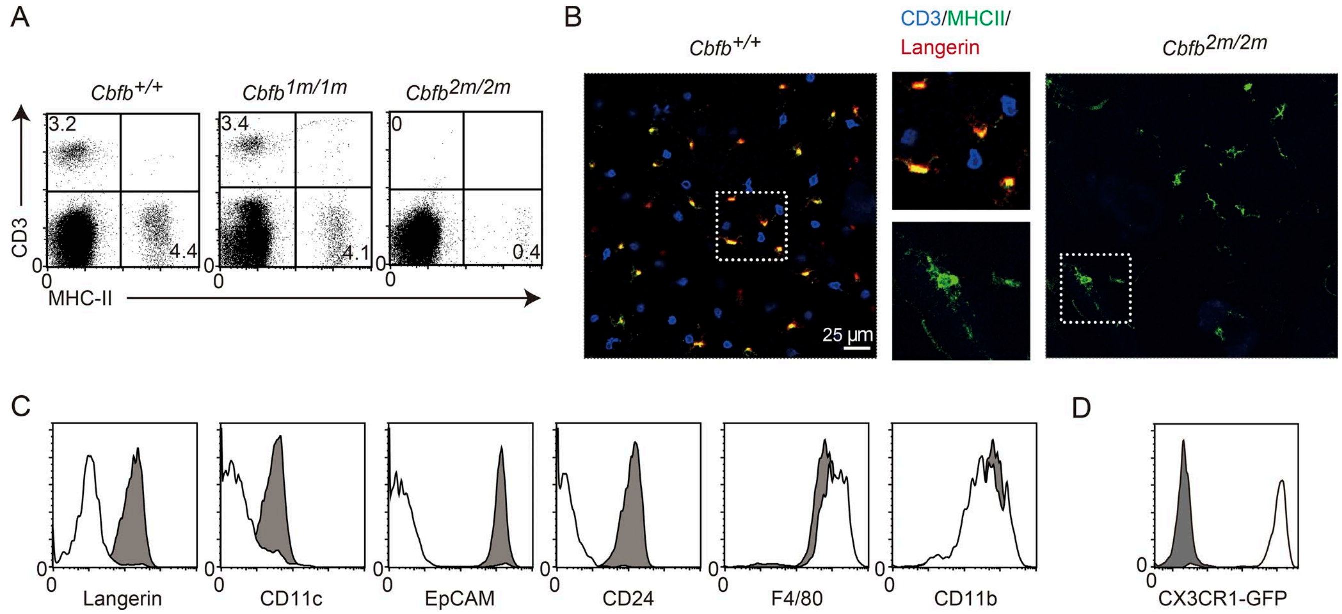

Figure 1. **LCs are absent in *Cbfb*$^{2m/2m}$ mice.** (A) Dot plots show representative CD3 and MHC-II expression in total epidermal cells of 2-mo-old *Cbfb*$^{+/+}$, *Cbfb*$^{1m/1m}$, and *Cbfb*$^{2m/2m}$ mice. One representative of at least five mice. (B) Images of immunohistochemistry show epidermal sheets from 2-mo-old *Cbfb*$^{+/+}$ and *Cbfb*$^{2m/2m}$ mice stained with CD3 (blue), MHC-II (green), and Langerin (red). Enlarged views of the area marked with a dotted square are shown in the middle. One representative of three experiments. (C) Histograms show the expression of Langerin, CD11c, EpCAM, CD24, F4/80, and CD11b on epidermal MHC-II$^+$ cells in *Cbfb*$^{+/+}$ (shaded) and *Cbfb*$^{2m/2m}$ (open) mice. One representative of five mice. (D) Histograms show the expression of CX3CR1-GFP on CD45$^+$CD3$^-$MHC-II$^+$ cells from *Cbfb*$^{+/+}$:*Cx3cr1*$^{+/gfp}$ (shaded) and *Cbfb*$^{2m/2m}$:*Cx3cr1*$^{+/gfp}$ (open) epidermis tissues. Results shown represent at least three separate experiments.

MHC-II from both *Cbfb*$^{+/+}$ and *Cbfb*$^{2m/2m}$ mice (Fig. 2, B and C). Consistent with this finding, *Cbfb1* and *Cbfb2* expression was increased on the P4 MHC-II$^+$EpCAM$^+$ population (Fig. S1). By P3, as expected, an MHC-II$^+$EpCAM$^+$ population lacking CX3CR1 expression emerged from *Cbfb*$^{+/+}$ mice; however, we could not detect any cells with this phenotype from *Cbfb*$^{2m/2m}$ mice. By P7, nearly all LC-lineage CD45$^+$CD3$^-$CD11b$^+$F4/80$^+$ cells from *Cbfb*$^{+/+}$ mice expressed MHC-II, and 75% of these differentiated into EpCAM$^+$ cells. In contrast, in the epidermis of P7 *Cbfb*$^{2m/2m}$ mice, the MHC-II$^+$EpCAM$^-$ subset represented the largest population, and MHC-II$^-$EpCAM$^-$ precursors were still present. In 1-mo-old *Cbfb*$^{2m/2m}$ mice, the accumulation of MHC-II$^+$EpCAM$^-$ cells was even more apparent, and MHC-II$^-$EpCAM$^-$ precursors were no longer detectable. These results indicated that Cbfβ2 ablation leads to developmental arrest during the transition from the MHC-II$^+$EpCAM$^-$ (precursor LC) to the MHC-II$^+$EpCAM$^+$ (mature LC) stage.

Late LC differentiation can occur from Gr-1$^+$ monocytes recruited to the *Cbfb*$^{2m/2m}$ epidermis

Despite the observed developmental block during the *Cbfb*$^{2m/2m}$ postnatal period, we noted that some MHC-II$^+$EpCAM$^+$ cells emerged in the epidermis from 4-mo-old *Cbfb*$^{2m/2m}$ mice (Fig. 2, B and C). Importantly, these MHC-II$^+$EpCAM$^+$ cells were negative for CX3CR1 expression (Fig. 2 B), suggesting that they were not LC precursors. Analyses of other relevant markers revealed that these MHC-II$^+$EpCAM$^+$ cells express Langerin, CD24, and CD11c (Fig. 3 A). In addition, they were smaller in size than the MHC-II$^+$EpCAM$^-$ subset (Fig. 3 A). Thus, we phenotypically and morphologically characterized these cells as mature LCs.

Previous studies showed that circulating Gr-1$^+$ monocytes, which are derived from BM progenitors, migrate to the epidermis and give rise to LCs in LC-depleted or -deficient epidermis (Ginhoux et al., 2006; Seré et al., 2012). Given the arrest of LC differentiation and the low numbers of LC-lineage cells in the epidermis of *Cbfb*$^{2m/2m}$ mice, we speculated that an influx of Gr-1$^+$ monocytes into the epidermis of adult *Cbfb*$^{2m/2m}$ mice occurs, even during steady states. Indeed, Gr-1$^+$MHC-II$^-$ cells were detected in CD45$^+$CD3$^-$CD11b$^+$ epidermal populations as soon as 1 mo after birth in *Cbfb*$^{2m/2m}$ mice (Fig. 3 B). These epidermal Gr-1$^+$ cells expressed lower levels of F4/80 than MHC-II$^+$ cells (Fig. 3 B). The percentage of Gr-1$^+$ cells in the CD45$^+$CD3$^-$CD11b$^+$ epidermal population increased by up to 20% from 1 to 4 mo after birth, whereas these cells were almost undetectable in the *Cbfb*$^{+/+}$ epidermis (Fig. 3 B). These results not only suggested that mature LCs could emerge from Gr-1$^+$ monocytes, but also raised questions regarding the origin of MHC-II$^+$EpCAM$^-$ LC precursor-like cells in the epidermis of adult *Cbfb*$^{2m/2m}$ mice.

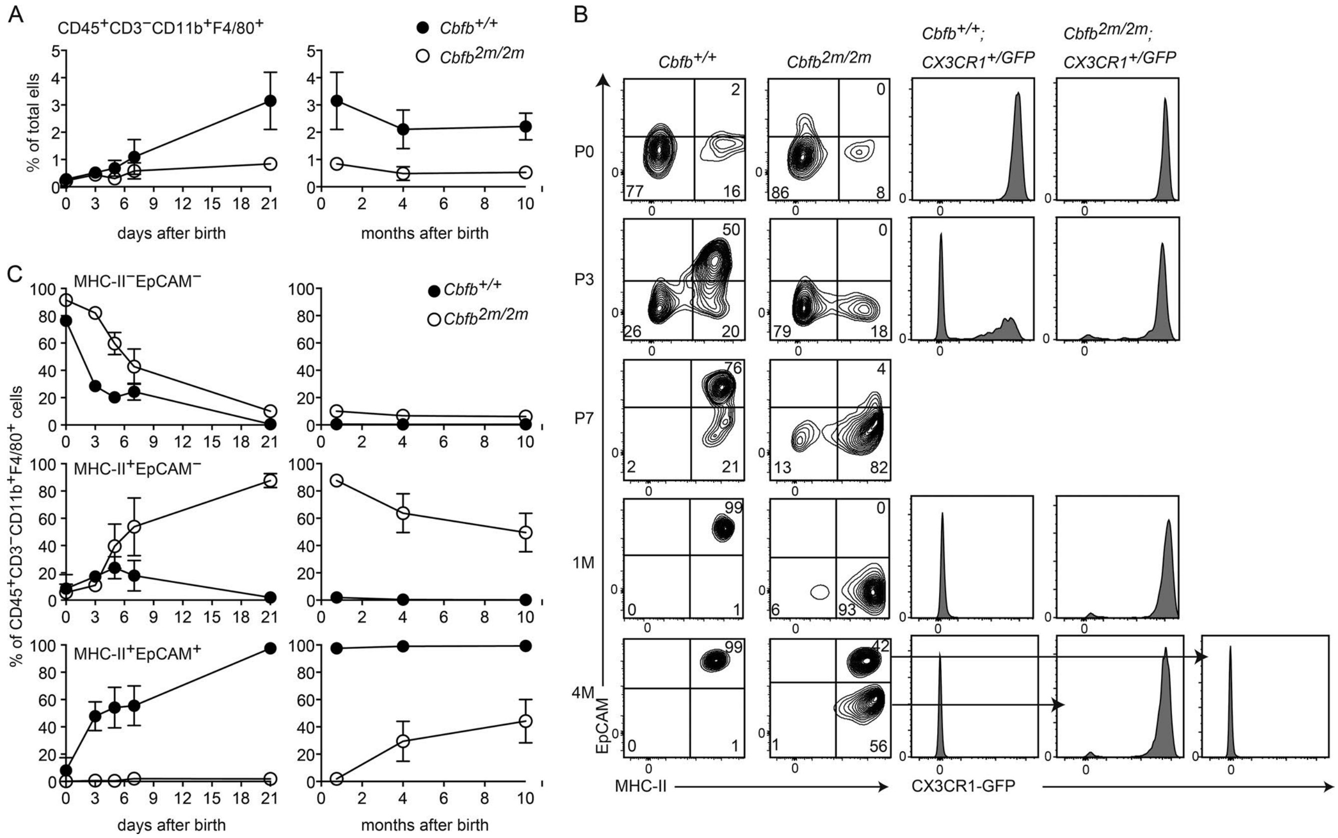

Figure 2. **LC differentiation from precursors was arrested at the transition to the EpCAM⁺ stage with Cbfβ2 ablation.** (A) Graphs show percentage of CD45⁺CD3⁻CD11b⁺F4/80⁺ cells in total epidermal cells of *Cbfb$^{+/+}$* (●) and *Cbfb$^{2m/2m}$* (○) mice at the indicated days (left) and months (right) after birth. Results from at least three mice are shown as means ± SD. (B) Contour plots show the expression of MHC-II and EpCAM on CD45⁺CD3⁻CD11b⁺F4/80⁺ epidermal cells of *Cbfb$^{+/+}$* and *Cbfb$^{2m/2m}$* mice. Histograms show CX3CR1-GFP expression in CD45⁺CD3⁻CD11b⁺F4/80⁺ epidermal cells. Because both MHC-II⁺EpCAM⁺ and MHC-II⁺EpCAM⁻ cells were present in 4-mo-old *Cbfb$^{2m/2m}$* mice, CX3CR1-GFP expression in each cell subset is shown in a separate histogram. (C) Graphs show kinetic changes in the proportions of MHC-II⁻EpCAM⁻, MHC-II⁺EpCAM⁻, and MHC-II⁺EpCAM⁺ subsets in the epidermal CD45⁺CD3⁻CD11b⁺F4/80⁺ population of *Cbfb$^{+/+}$* (●) and *Cbfb$^{2m/2m}$* (○) mice at the indicated days (left) and months (right) after birth. Results from at least three mice are shown as means ± SD.

Immature LC precursor–like cells persist in the epidermis of *Cbfb$^{2m/2m}$* mice

Radioresistance of LCs is a hallmark of their embryonic ontogeny (Merad et al., 2002). To further characterize the MHC-II⁺EpCAM⁻ cells in adult *Cbfβ$^{2m/2m}$* mice, we performed a BM chimera experiment using CD45.1⁺ wild-type BM cells injected into sublethally irradiated CD45.2⁺ *Cbfb$^{+/+}$* or CD45.2⁺ *Cbfb$^{2m/2m}$* recipient mice. 7 mo later, nearly all CD11c⁺ DCs in the spleen of both *Cbfβ$^{+/+}$* and *Cbfβ$^{2m/2m}$* recipients expressed the donor marker CD45.1 (Fig. 4 A). In contrast, the majority of LCs were of host origin (CD45.2) in *Cbfβ$^{+/+}$* recipient animals (Fig. 4 A). However, in the epidermis of *Cbfb$^{2m/2m}$* recipient mice, 25% of the MHC-II⁺ population was of donor origin, suggesting that these donor cells were derived from donor Gr-1⁺ blood monocytes. Importantly, the majority of the MHC-II⁺ population with immature characteristics such as low Langerin expression remained of host origin (CD45.2) and consisted of LC precursors that exhibited radioresistance and tissue-residency properties of bona fide skin-residential LCs.

To examine tissue residency in noninflammatory conditions, we performed parabiosis experiments, in which parabionts shared the same blood circulation, allowing exchange of hematopoietic cells between them (Merad et al., 2002). After 7 mo, the splenic CD11c⁺ population of each parabiont consisted equally of CD45.1⁺ and CD45.2⁺ cells in both CD45.1⁺ *Cbfb$^{+/+}$*:CD45.2⁺ *Cbfb$^{+/+}$* and CD45.1⁺ *Cbfb$^{+/+}$*:CD45.2⁺ *Cbfb$^{2m/2m}$* pairs (Fig. 4 B). In contrast, the epidermal MHC-II⁺ population was hardly exchanged in the CD45.1⁺ *Cbfβ$^{+/+}$*:CD45.2⁺ *Cbfb$^{+/+}$* pair, and CD45.1- and CD45.2-expressing cells were detected only in the epidermis of CD45.1 and CD45.2 parabionts, respectively (Fig. 4 B). In sharp contrast, a significant number of CD45.1⁺ cells showing characteristics of mature LCs were detected in the epidermis of CD45.2⁺ *Cbfb$^{2m/2m}$* parabionts

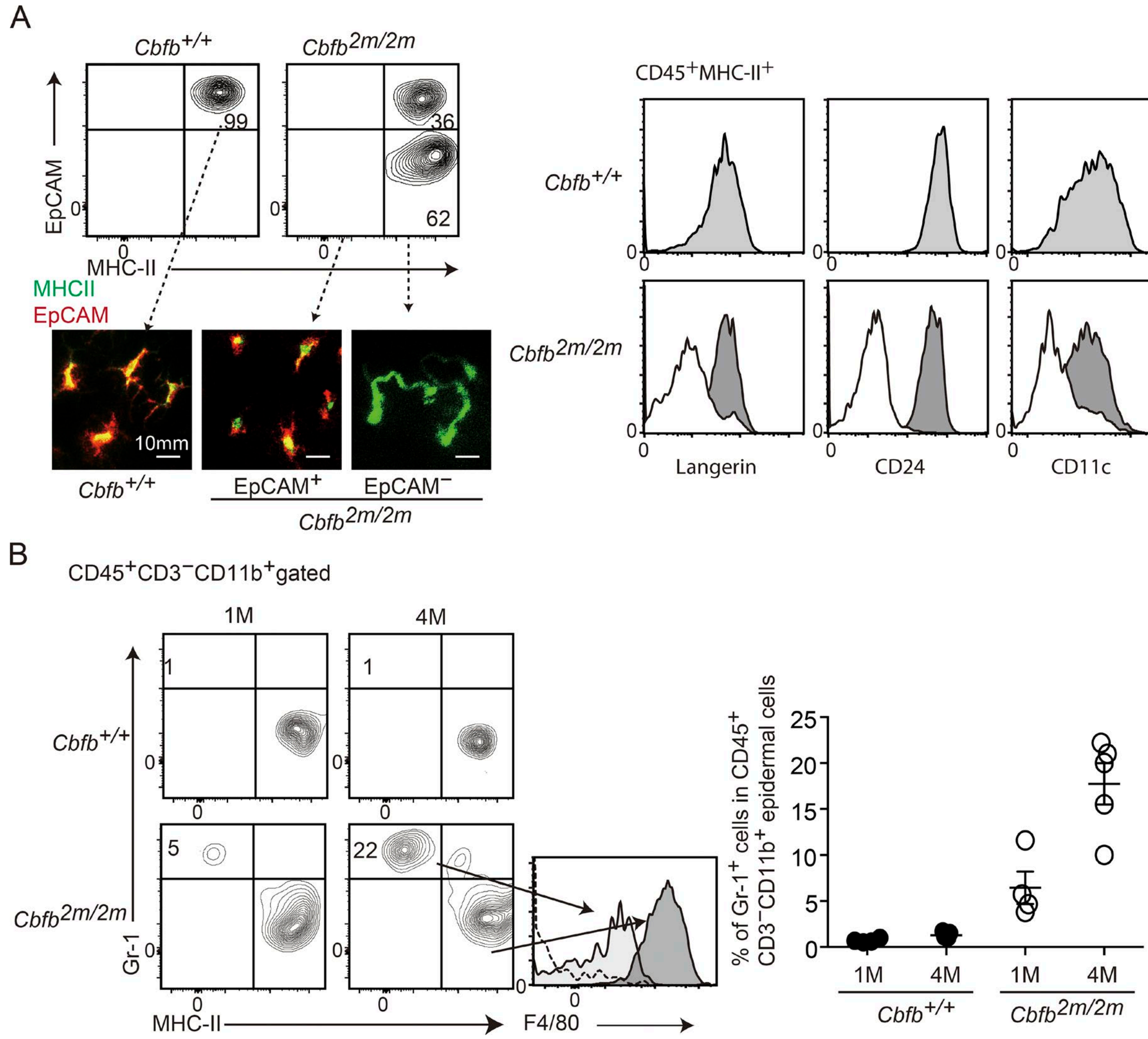

Figure 3. **Emergence of Gr-1$^+$ monocyte-derived LCs in the epidermis of older *Cbfb*$^{2m/2m}$ mice.** (A) Contour plots show the expression of MHC-II and EpCAM on CD45$^+$CD3$^-$CD11b$^+$F4/80$^+$ epidermal cells (left top), and representative immunohistochemistry images show the expression of MHC-II (green) and EpCAM (red) on epidermal sheets from 4-mo-old *Cbfb*$^{+/+}$ and *Cbfb*$^{2m/2m}$ mice (left bottom). Histograms show the expression of Langerin, CD24, and CD11c on epidermal CD45$^+$MHC-II$^+$EpCAM$^+$ cells (shaded) and CD45$^+$MHC-II;EpCAM$^-$ (open) cells from 4-mo-old *Cbfb*$^{+/+}$ and *Cbfb*$^{2m/2m}$ mice. Results shown are representative of three separate experiments. (B) Contour plots show the expression of Gr-1 and MHC-II on CD45$^+$CD3$^-$CD11b$^+$ epidermal cells of 1- and 4-mo-old (1M and 4M) *Cbfb*$^{+/+}$ and *Cbfb*$^{2m/2m}$ mice. Histogram shows F4/80 expression on Gr-1$^+$ and MHC-II$^+$ populations from 4-mo-old *Cbfb*$^{2m/2m}$ mice. Open histograms indicate F4/80 expression on CD3$^+$ cells as a negative control. Graph shows a summary of the percentage of Gr-1$^+$ cells in CD45$^+$CD3$^-$CD11b$^+$ epidermal cells of at least four mice; means ± SD.

(Fig. 4 B), further supporting the contention that recruitment and differentiation from circulating Gr-1$^+$ monocytes into mature LCs takes place in the *Cbfb*$^{2m/2m}$ epidermis. However, we were still able to identify a significant population of host (CD45.2$^+$) MHC-II$^+$ cells that did not express any markers of maturation, such as EpCAM, CD24, and Langerin (Fig. 4 B).

Altogether, our observations indicated that Cbfβ2-deficient LC precursor-like cells retain properties of tissue residency, and homeostasis is maintained in an epidermal-specific manner, as was the case for mature LCs.

Persisting LC precursor–like cells in the epidermis of *Cbfb*$^{2m/2m}$ mice are embryonic derived

We next examined whether and to what extent embryonic-derived precursors survive throughout life and contribute to the maintenance of the MHC-II$^+$EpCAM$^-$ population in adult Cbfβ2-deficient mice. For this, we performed a fate-mapping experiment using a transgenic mouse line expressing the tamoxifen-inducible Mer-iCre fusion protein driven by the *Csf1r* promoter (Csf1r-iCre transgenic mice; Schulz et al., 2012). Injection of 4-hydroxytamoxifen (4-OHT) into pregnant animals at 8.5 dpc resulted in the

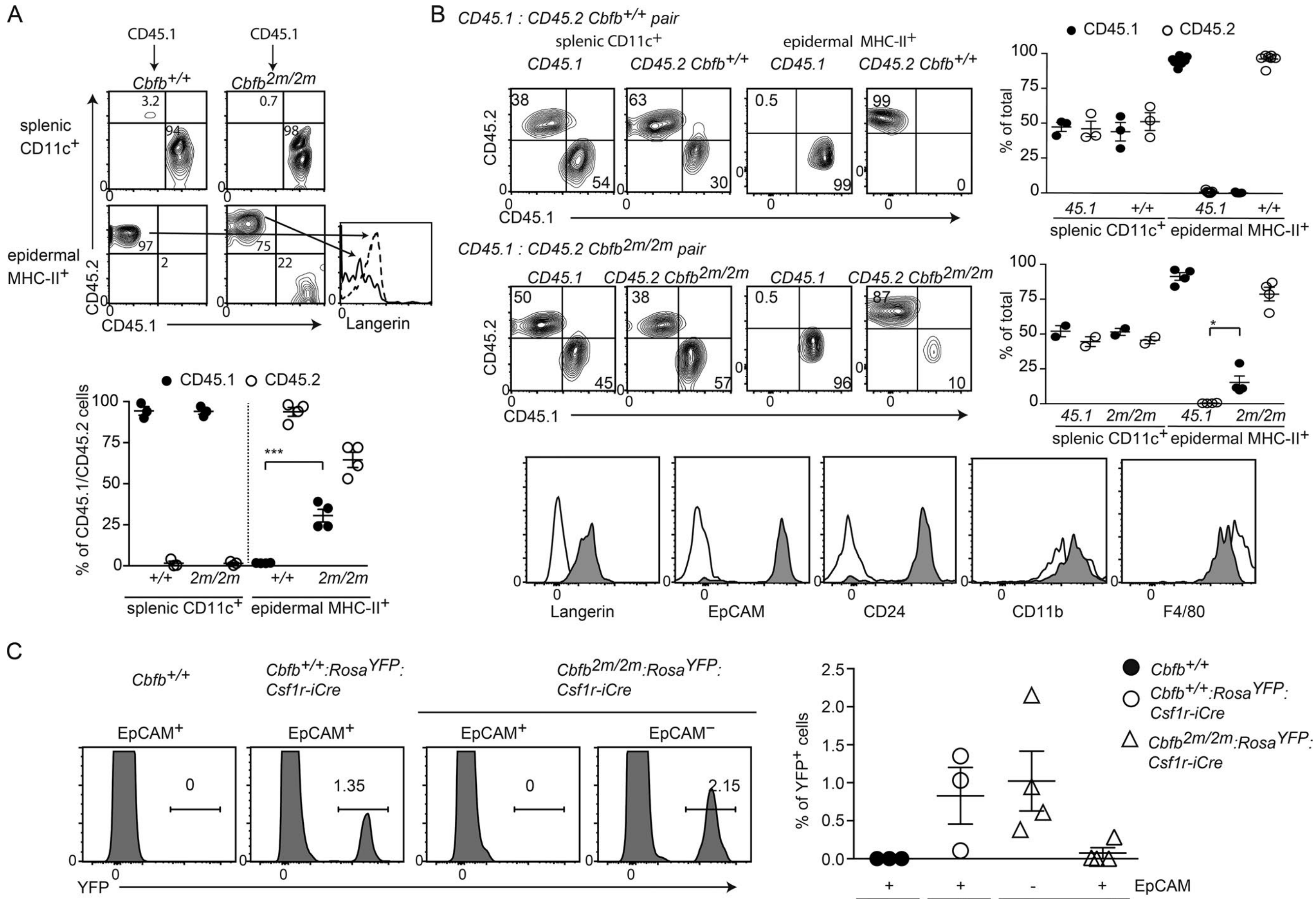

Figure 4. **Persistence of embryonic-derived immature LC precursors in the adult epidermis of *Cbfb*$^{2m/2m}$ mice.** (A) Contour plots show the expression of CD45.1 and CD45.2 in splenic CD11c$^+$ and epidermal MHC-II$^+$ populations in sublethally irradiated CD45.2 *Cbfb*$^{+/+}$ and CD45.2 *Cbfb*$^{2m/2m}$ recipients 7 mo after intravenous injection of CD45.1 BM. Histogram shows Langerin expression on CD45.2 *Cbfb*$^{+/+}$ (dashed line) and CD45.2 *Cbfb*$^{2m/2m}$ (solid line) cells. Graph shows the proportions of CD45.1$^+$ (●) and CD45.2$^+$ (○) cells in indicated cell populations of *Cbfb*$^{+/+}$ and *Cbfb*$^{2m/2m}$ recipients; means ± SD; ***, $P < 0.001$ (unpaired Student's *t* test). (B) Contour plots show the expression of CD45.1 and CD45.2 in indicated cell populations of each parabiont of CD45.1 *Cbfb*$^{+/+}$ and CD45.2 *Cbfb*$^{+/+}$ pair and CD45.1 *Cbfb*$^{+/+}$ and CD45.2 *Cbfb*$^{2m/2m}$ pair 7 mo after the establishment of parabiosis. Graph shows summarized proportions of CD45.1$^+$ (●) and CD45.2$^+$ (○) cells in indicated cell subsets of each parabiont of indicated pairs; means ± SD; *, $P < 0.01$ (unpaired Student's *t* test). Histograms show the expression of indicated markers on CD45.1$^+$ (shaded) and CD45.2$^+$ (open) epidermal MHC-II$^+$ cells of CD45.1 *Cbfb*$^{+/+}$ and CD45.2 *Cbfb*$^{2m/2m}$ pairs. One representative of at least four experiments. (C) Marking of yolk sac–derived cells of *Csf1r-iCre* transgenic mice. Histograms show YFP expression from the *Rosa26*^{YFP} reporter allele in EpCAM$^+$ and EpCAM$^-$ cells of 4-mo-old offspring of indicated genotypes from mothers that received a 4-OHT injection at 8.5 dpc. Graph shows a summary of the proportion of YFP$^+$ cells from at least three individual mice; means ± SD.

specific marking of embryonic macrophages and their progeny with YFP expression from the Rosa26-STOP-YFP allele (*Rosa26*^{YFP}; Schulz et al., 2012). We crossed *Cbfb*$^{+/2m}$ mice harboring both *Rosa26*^{YFP} and *Csf1r-iCre* transgenes, selected offspring according to the desired genotype, and examined them at 4 mo of age when both MHC-II$^+$EpCAM$^-$ and MHC-II$^+$EpCAM$^+$ populations should be present in the epidermis of *Cbfb*$^{2m/2m}$ mice (Fig. 2). In double transgenic mice, 1% of EpCAM$^+$ cells expressed YFP, a tagging efficiency similar to that reported previously (Schulz et al., 2012). In *Cbfb*$^{2m/2m}$ offspring, a similar percentage of YFP$^+$ cells was detected in MHC-II$^+$EpCAM$^-$ LC precursor-like cells, whereas no YFP-expressing cells were detected in epidermal MHC-II$^+$EpCAM$^+$ mature LCs (Fig. 4 C). These results strongly support that the MHC-II$^+$EpCAM$^-$ population is of embryonic origin and is likely to survive in the epidermis until adulthood.

MHC-II$^+$EpCAM$^-$ LC precursors lose developmental potential with time

We next examined whether MHC-II$^+$EpCAM$^-$ cells from adult *Cbfb*$^{2m/2m}$ mice retain the developmental potential to differentiate into mature LCs. Because of the lack of established methods available to induce LC differentiation from epidermal precursors in vitro, we tested whether restoration of Cbfβ2 expression in vivo could induce LC differentiation by

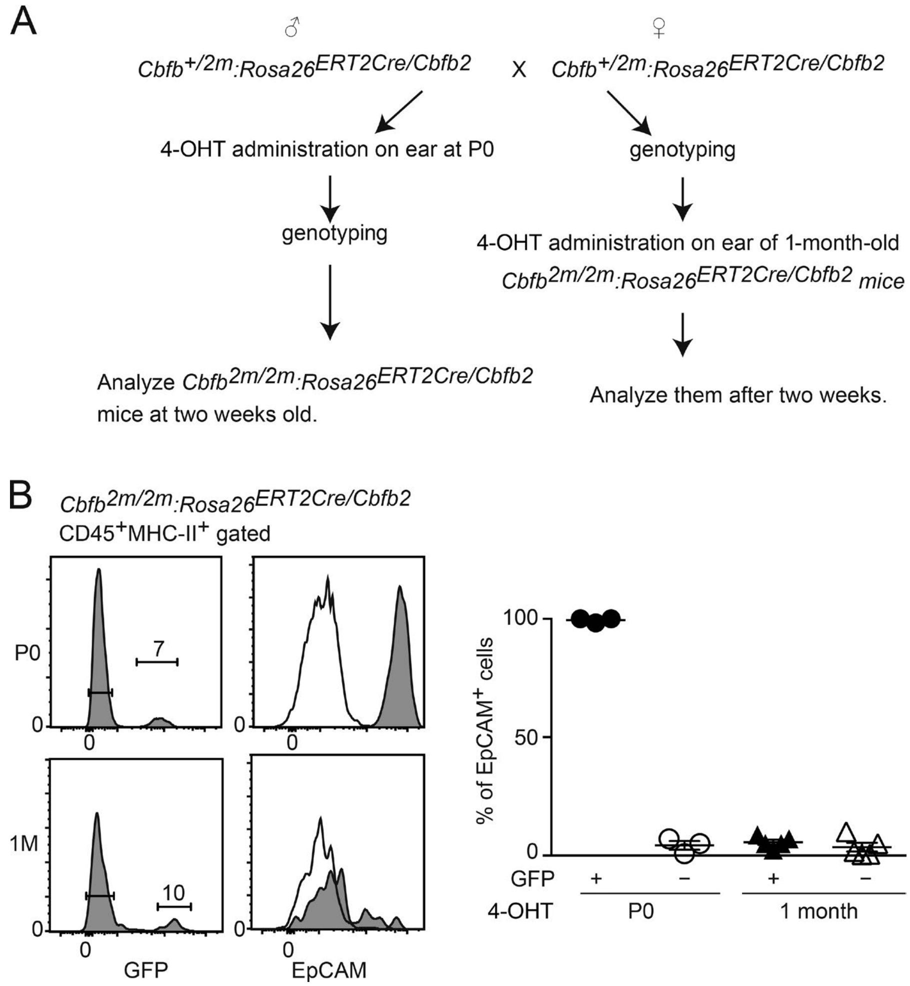

Figure 5. **Loss of developmental potency in skin-residential LC precursors of *Cbfb*$^{2m/2m}$ mice.** (A) Scheme shows the experimental flow for conditional expression of Cbfβ2 and the analyses of its effect on LC differentiation. Skin-specific activation of ERT2Cre expressed from the *Rosa26*^{ERT2Cre} allele by topical administration of 4-OHT induced Cbfβ2 expression from the *Rosa26*^{Cbfb2} locus, which could be traced by GFP expression from this locus. 2 wks after the first 4-OHT treatment (P0 or 1 mo [1M]), mice were killed to analyze GFP and EpCAM expression in CD45$^+$MHC-II$^+$ cells. (B) Histograms show GFP expression in CD45$^+$MHC-II$^+$ cells (left) and EpCAM expression in GFP$^+$ (shaded) and GFP$^-$ (open) cells from *Cbfb*$^{2m/2m}$:*Rosa26*$^{ERT2Cre/Cbfb2}$ mice. Graph shows a summary of three independent experiments; means ± SD. EpCAM expression was induced from Cbfβ2-deficient CD45$^+$ MHC-II$^+$ cells upon rescue of Cbfβ2 expression at P0, but not at 1M.

establishing another mouse strain in which Cbfβ2 expression could be induced from the *Rosa26* locus after Cre-mediated excision of STOP signals (a *Rosa26*^{Cbfb2} locus). The presence of internal ribosome entry site GFP sequences downstream of *Cbfb2* cDNA in the *Rosa26*^{Cbfb2} allele allowed us to identify cells expressing transgenic Cbfβ2 by tracing reporter GFP expression. The *Rosa26*^{Cbfb2} mouse strain was crossed with another transgenic strain expressing the Mer-iCre fusion protein from the *Rosa26* locus (a *Rosa26*^{ERT2} locus) and was sequentially crossed with *Cbfb*$^{2m/2m}$ mice. To obtain newborn mice harboring the *Cbfb*$^{2m/2m}$:*Rosa26*$^{ERT2Cre/Cbfb2}$ genotype, we crossed *Cbfb*$^{+/2m}$:*Rosa26*$^{ERT2Cre/Cbfb2}$ mice (Fig. 5 A).

We performed two sets of experiments, one with restored Cbfβ2 expression at birth representing "normal" development and one with restoration at a later stage in adult animals. First, we administered 4-OHT for 5 d from P0 and analyzed the epidermal content after 2 wks. GFP$^+$ cells were detected from ~10% of CD45$^+$MHC-II$^+$cells (Fig. 5 B) as well as from 0.4% of CD45$^-$ cells (Fig. S2 A). In this experimental setting, there were no GFP$^+$ hematopoietic cells detected in CD11b$^+$ blood monocytes (Fig. S2 B), confirming the skin-specific induction of Cbfβ2 by topical 4-OHT administration. Importantly, all GFP$^+$ cells in the CD45$^+$MHC-II$^+$ population became EpCAM$^+$ cells (Fig. 5 B), indicating that the induction of Cbfβ2 when LC differentiation normally occurs is enough to restore LC development in *Cbfb*$^{2m/2m}$ mice. Second, we topically administered 4-OHT to 4-wk-old *Cbfb*$^{2m/2m}$ mice for 5 d. In contrast to administration at P0, transgenic Cbfβ2 expression at 4 wks, which was confirmed by reporter GFP expression in 10% of CD45$^+$ cells, failed to induce EpCAM$^+$ expression in CD45$^+$MHC-II$^+$ cells (Fig. 5 B). This result indicated that, at least in terms of EpCAM induction, epidermal resident *Cbfb*$^{2m/2m}$ MHC-II$^+$EpCAM$^-$ cells lost their developmental ability to mature after 1 mo.

Altered gene expression profiles in MHC-II$^+$EpCAM$^-$ LC precursors

To gain insights into the molecular basis of the diminishing developmental potency of epidermal-residual LC precursors in *Cbfb*$^{2m/2m}$ mice, we prepared epidermal CD45$^+$CD3$^-$MHC-II$^+$ cells from P5 and 1.5-mo-old animals (referred hereafter to as postnatal and adult, respectively) and compared gene expression profiles between

Cbfb$^{+/+}$ and *Cbfb*$^{2m/2m}$ mice using barcode-based digital RNA sequences (Shiroguchi et al., 2012). We found more than 400 differentially expressed genes among four cell subsets (Fig. S3 A), and primary component analyses showed that these four subsets clustered separately (Fig. 6 A). According to PC1 values, postnatal cells were relatively close to each other. Some genes including *Smad7*, encoding inhibitory Smad, and *Runx3* are commonly up-regulated in control LCs and adult *Cbfb*$^{2m/2m}$ LC precursors (Fig. S3 B). In addition, comparing combinatorial gene expression changes between postnatal and adult *Cbfb*$^{2m/2m}$ cells with regard to cytokine–receptor pairs showed that the expression of both *Tgfbr1* and *Tgfbr2* was elevated in adult *Cbfb*$^{2m/2m}$ cells (Figs. 6 B and S3, C and D). In adult *Cbfb*$^{2m/2m}$ cells, the expression of *Tgfb1* was maintained at the same level as in postnatal cells (Fig. 6 B). In addition, adult *Cbfb*$^{2m/2m}$ cells expressed higher levels of *Lamtor2*, which encodes a component of LAMTOR complexes that transmit TGFβ1 signals (Sparber et al., 2015), and Axl, which transduces signals that result in the preservation of a quiescent state (Bauer et al., 2012; Fig. S3 D). This suggested that the TGFβR1 pathway, which is required to maintain a quiescent state, is functionally enhanced in these cells. In contrast, the *Bmp7-Bmpr1a* transcript pair was reduced in adult *Cbfb*$^{2m/2m}$ cells compared with postnatal *Cbfb*$^{2m/2m}$ cells (Fig. 6 B). In addition, levels of the *Ctnnb1* transcript were reduced in adult *Cbfb*$^{2m/2m}$ cells (Fig. S3 D). This gene encodes β-catenin and is induced by TGFβ1 to promote LC differentiation synergistically with vitamin D receptor (VDR; Yasmin et al., 2013b). Interestingly, the expression of *Vdr* was also reduced in adult *Cbfb*$^{2m/2m}$ cells (Fig. S3 D). These results indicated that postnatal and adult *Cbfb*$^{2m/2m}$ cells have district gene expression signatures, particularly related to TGFβ superfamily signaling, with high and low expression of the *Tgfb-Tgfbr1* and *Bmp7-Bmpr1a* axes, respectively, in adult cells.

BMP signaling is important for LC functional differentiation

To examine the function of Cbfβ2 in TGFβR signaling during LC differentiation, BM progenitors were cultured with TGFβ1 and GM-CSF, a cytokine combination that induces LC-like cell development (Chopin et al., 2013). After 3 d of culture, CD205^{+}EpCAM^{+} LC-like cells were differentiated from *Cbfb*$^{+/+}$ BM progenitors. However, the differentiation of CD205^{+}EpCAM^{+} cells from *Cbfβ*$^{2m/2m}$ progenitors was markedly inefficient (Fig. 6 C). Furthermore, the differentiation of CD205^{+}EpCAM^{+} cells was impaired by dorsomorphin, an inhibitor of BMP type I receptors including BMPR1A, but not by SB431542, an inhibitor of TGFβR1. These observations confirmed that signaling through BMPR1A is more important for LC differentiation.

Consistent with the retention of *Cbfβ*$^{2m/2m}$ LC precursors in the adult epidermis, the expression of CD40, CD86, and CCR7, which is induced by loss of TGFβR1 signaling and involved in LC egress from the epidermis (Kel et al., 2010), was comparable between *Cbfb*$^{+/+}$ and *Cbfb*$^{2m/2m}$ cells (Fig. 6 D). Altogether, these observations suggested that reduced expression of *Bmpr1a* diminishes the developmental potential of embryonic *Cbfb*$^{2m/2m}$ LC precursors, whereas the migratory capacity required for epidermal egress is inhibited by enhanced TGFβR1 signaling (Fig. 6 E).

Role of Runx3/Cbfb complexes during LC differentiation

A previous study reported the absence of MHC-II^{+} cells in the Runx3-deficient epidermis (Fainaru et al., 2004). Because Runx3 must interact with Cbfβ to exert its function, a discrepancy in presence or absence of epidermal MHC-II^{+} cells between Runx3- and Cbfβ2-deficient mice could be explained by the functional redundancy of Cbfβ1. We therefore examined the effect of total ablation of Cbfβ function in DC-lineage cells using *Cbfb*$^{F/F}$*:CD11c-Cre* mice. Although the CD45^{+}MHC-II^{+} population was significantly reduced in the epidermis of *Cbfb*$^{F/F}$*:CD11c-Cre* mice, one third of these cells were present as MHC-II^{+} EpCAM^{-} LCs (Fig. 7 A). These MHC-II^{+}EpCAM^{-} cells did not up-regulate CD86 or CCR7 expression (Fig. 7 B), indicating that the maintenance of a quiescent state by TGFβR1 signaling is likely independent of Cbfβ. This observation not only suggested that MHC-II^{+} LC precursors could be present in Runx3-deficient mice, but also indicated that Runx3/Cbfβ2 complexes have a unique role in transmitting selective signals through BMPR1A during stimulation by the TGFβ superfamily.

DISCUSSION

Our observations provide several novel insights into the underlying mechanisms through which the LC network is established and maintained. In this study, we first unraveled a unique role for Cbfβ2 in establishing the epidermal LC network. We showed that in Cbfβ2-deficient mice, embryonic-derived LC precursors can persist in the epidermis until adulthood through impaired selective TGFβ superfamily signaling, which is essential for LC differentiation. However, the conditional rescue of Cbfβ2 expression also revealed that such epidermal-resident Cbfβ2-deficient LC precursors do not maintain developmental potency.

It is widely accepted that inhibition of the TGFβ1/TGFβR1 pathway leads to the depletion of LCs in the adult epidermis. Initially, the simplest interpretation was that TGFβ1 is essential for LC differentiation, specifically to drive embryonic LC precursors to differentiate into the EpCAM^{+}/Langerin^{+} stage (Borkowski et al., 1996; Kaplan et al., 2007; Chorro et al., 2009; Nagao et al., 2009). However, other studies subsequently revealed that signaling through TGFβR1 has another role in the maintenance of a quiescent state in LCs (Kel et al., 2010; Bobr et al., 2012), specifically, promoting their retention in the epidermis. It was proposed that these two pathways, LC differentiation and maintenance in a quiescent state, are likely to

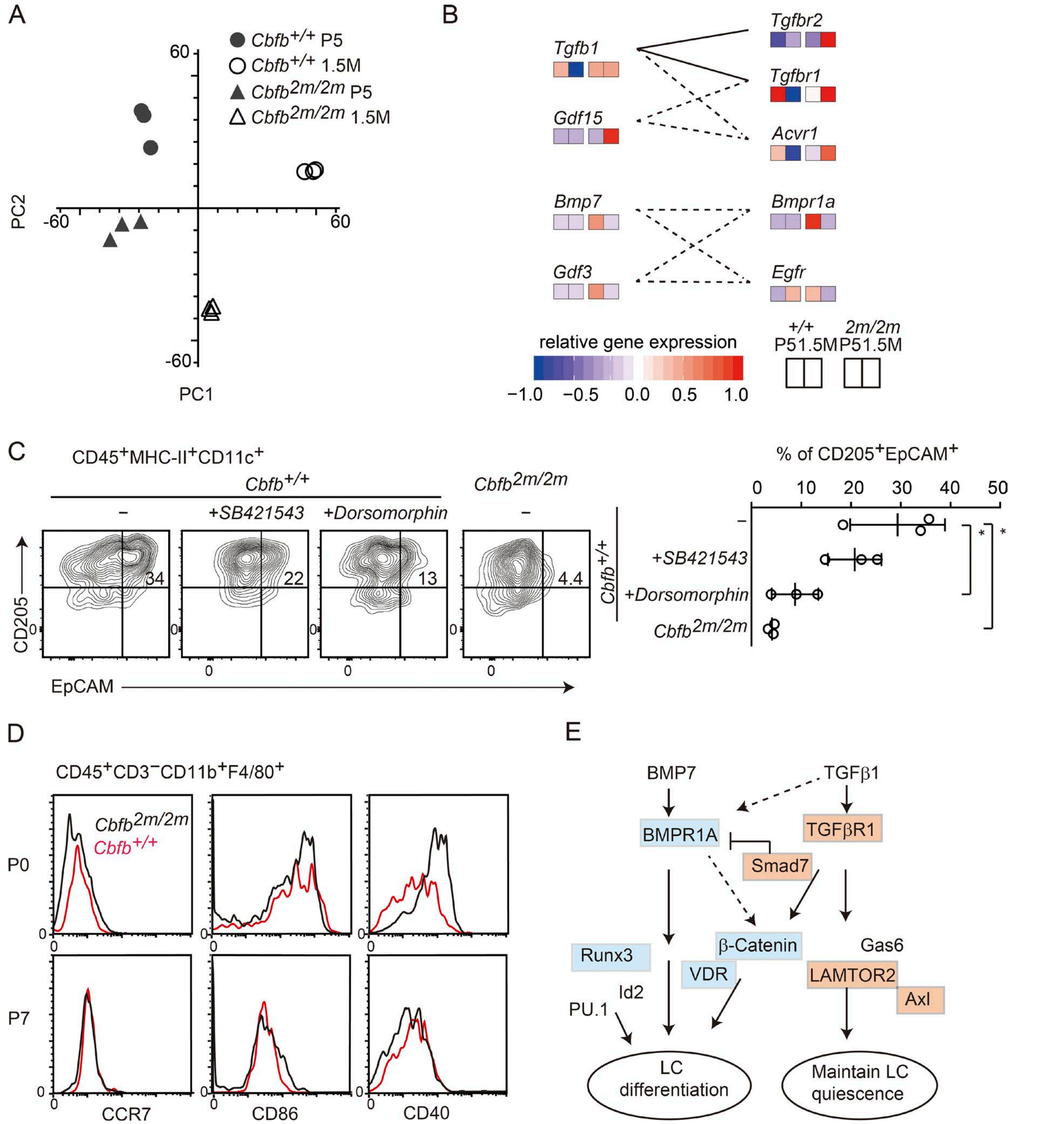

Figure 6. **Altered gene expression signatures of skin-resident *Cbfb*$^{2m/2m}$ LC precursors at 1 mo.** (A) Principle component analyses of digital RNA-seq data from CD45$^+$CD3$^-$MHC-II$^+$ epidermal cells prepared from P5 and 1.5-mo-old (1.5M) *Cbfb*$^{+/+}$ and *Cbfb*$^{2m/2m}$ mice. (B) Selective cytokine–receptor pair expression. *Bmp7-Bmpr1a* and *Tgfb1-Tgfbr1* pairs exhibited opposite directional changes between P5 and 1.5M in *Cbfb*$^{2m/2m}$ CD45$^+$CD3$^-$MHC-II$^+$ cells. (C) Differentiation of LC-like cells from BM progenitors in vitro. Lineage-negative BM progenitors from *Cbfb*$^{+/+}$ and *Cbfb*$^{2m/2m}$ mice were cultured for 3 d in the presence of GM-CSF and TGFβ with or without SB421543 and dorsomorphin. Dot plot shows EpCAM and CD205 expression on CD45$^+$MHC-II$^+$CD11c$^+$ cells. Numbers indicate the percentage of CD205$^+$EpCAM$^+$ subset. Graph summarizes the proportion of CD205$^+$EpCAM$^+$ cells in the CD45$^+$MHC-II$^+$CD11c$^+$ population from three experiments; means ± SD; *, $P < 0.01$ (unpaired Student's *t* test). (D) Histogram shows the expression of CCR7, CD86, and CD40 on CD45$^+$CD3$^-$CD11b$^+$ epidermal cells of *Cbfb*$^{+/+}$ (red) and *Cbfb*$^{2m/2m}$ (black) mice. Results are representative of at least three individual mice. (E) Schematic summary of two cellular signaling pathways arising from TGFβ superfamily stimulation. Molecules expressed at higher and lower levels in adult LCs compared with expression in postnatal *Cbfb*$^{2m/2m}$ LC precursors are marked with orange and blue squares, respectively.

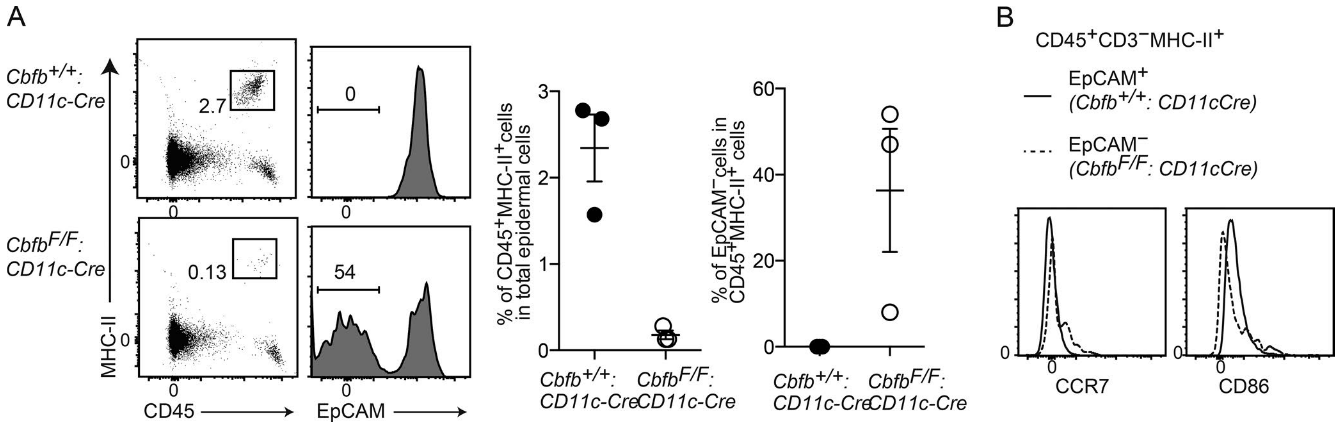

Figure 7. **Persistence of MHC-II$^+$ cells after complete loss of Cbfβ expression.** (A) Dot plots show the expression of MHC-II and CD45 on total epidermal cells, and histograms show EpCAM expression on CD45$^+$MHC-II$^+$ epidermal cells from 4-mo-old *Cbfb$^{+/+}$:CD11c-Cre* and *Cbfb$^{F/F}$:CD11c-Cre* mice. Numbers indicate the percentage of cells in the indicated gates. Graphs show the percentages of CD45$^+$MHC-II$^+$ cells in the total population of epidermal cells and the proportion of EpCAM$^-$ cells in CD45$^+$MHC-II$^+$ cells of *Cbfb$^{+/+}$:CD11c-Cre* (●) and *Cbfb$^{F/F}$:CD11c-Cre* (○) mice. Results are representative of at least three individual mice and are shown as means ± SD. (B) Histogram shows the expression of CCR7 and CD86 on CD45$^+$CD3$^-$CD11b$^+$ epidermal cells of *Cbfb$^{+/+}$:CD11c-Cre* (solid) and *Cbfb$^{F/F}$:CD11c-Cre* (dotted) mice. One representative of three individual mice.

be regulated by different TGFβ superfamily receptor pairs. Whereas BMP7-BMPR1A plays a prominent role in LC differentiation, TGFβ1-TGFβR1 signaling is crucial for the inhibition of LC activation and the retention of these cells in the epidermis (Kel et al., 2010; Yasmin et al., 2013a). Here we found that the expression of *Lamtor2* and *Axl*, which are involved in maintaining a quiescent state downstream of TGFβR1 signaling, was increased in skin-resident LC precursors of adult *Cbfb$^{2m/2m}$* mice. In contrast, expression of *Bmpr1a*, which is involved in LC differentiation, was reduced. Therefore, our results suggest that the selective inhibition of BMPR1A-dependent signaling, through the loss of Cbfβ2, inhibited LC differentiation when intact TGFβR1-mediated signals were present to preserve a quiescent state. Consequently, Cbfβ2-deficient LC precursors persisted in the epidermis.

EpCAM was previously shown to increase the motility of LCs in vivo (Gaiser et al., 2012). In this regard, it is possible that defective EpCAM expression in *Cbfb$^{2m/2m}$* LC precursors is involved in an additional mechanistic level of epidermal retention. However, given that TGFβR1-deficient LC precursors lacking EpCAM expression migrated out from the epidermis (Kel et al., 2010), it seems that TGFβR1 signaling rather than EpCAM expression drives LC retention in the epidermis. Although this model for distinct roles among TGFβ superfamily members predicts that BMP7- or BMPR1A-deficient mice should retain MHC-II$^+$ LC precursors in the adult epidermis, similar to what was observed in this study using Cbfβ2-deficient mice, neonatal or embryonic lethality of these mice (Mishina et al., 1995; Zouvelou et al., 2009) limited such analysis.

Our results also revealed that Cbfβ1 and Cbfβ2 have distinct roles in TGFβR signaling. First, Cbfβ1 could not compensate for loss of Cbfβ2 function, which is necessary for LC differentiation. The presence of MHC-II$^+$EpCAM$^-$ LC precursors in *Cbfb$^{f/f}$:CD11c-Cre* mice, in which the function of Cbfβ is completely abrogated, suggests that such LC precursors could similarly be present in the epidermis of adult Runx3-deficient mice. These observations tempted us to speculate that Runx3/Cbfβ complexes are not essential for the transmission of signals that are essential for the maintenance of LCs in a quiescent state during TGFβR1 signaling, although the Cbfβ-independent function of Runx3 in this regulation was not formally excluded. Given that Runx proteins interact with Smad proteins (Ito and Miyazono, 2003), Smad family proteins potentially interact with Runx3/Cbfβ2 complexes to regulate LC differentiation during BMP7-BMPR1A signaling. Although Smad2, Smad3, and Smad4 are not required for LC differentiation in vivo (Xu et al., 2012; Li et al., 2016; Zhang et al., 2016), it has been reported that BMP7 induces phosphorylation of Smad1/5/8 proteins in vitro (Yasmin et al., 2013a). Thus, these Smad1/5/8 proteins might be involved in transmitting signaling from BMPR1A to induce LC differentiation. Alternatively, it is possible that Runx3/Cbfβ2 complexes regulate LC differentiation during BMP7 stimulation in a Smad-independent manner. Understanding the molecular basis of Cbfβ2-dependent LC differentiation will require the identification of molecules that interact specifically with Cbfβ2.

We showed that *Cbfb$^{2m/2m}$* LC precursors can reside in the epidermis but fail to retain maturation potential upon rescue by Cbfβ2 expression. Our transcriptome analysis showed that expression of the TGFβ1-TGFβR1 axis was higher in adult *Cbfb$^{2m/2m}$* LC precursors. Although it remains unclear whether negative feedback regulation could restrain this axis, it is possible that the loss of Cbfβ2 might interfere with this process, resulting in enhanced TGFβR1 expression. In contrast, the expression of *Ctnnb1*, which is also induced by TGFβ1 stimulation in vitro in human $CD34^+$ hematopoietic progenitor cells (Yasmin et al., 2013b), was reduced in adult $Cbfb^{2m/2m}$ LC precursors. Thus, responsiveness to TGFβ1 might differ among putative TGFβ target genes in Cbfβ2-deficient LC precursors. Alternatively, the induction of *Ctnnb1* by TGFβ1 is mediated by receptors other than TGFβR1, such as BMPR1A. It is also possible that continuous exposure to TGFβ1 stimulation decreases responsiveness to TGFβ1 stimulation at certain gene loci such as *Ctnnb1*. As such, it was previously reported that forced expression of β-catenin in $CD34^+$ hematopoietic progenitor cells accelerates LC differentiation, and this effect was enhanced by VDR activity (Yasmin et al., 2013b). Interestingly, $Cbfb^{2m/2m}$ LC precursors in the adult epidermis exhibited reduced expression of *Ctnnb1* and *Vdr*, suggesting that the loss of these molecules, combined with low BMPR1A expression, is involved in the diminished maturation potential of $Cbfb^{2m/2m}$ LC precursors. It will be of interest to determine whether the down-regulation of these molecules arises from continuous TGFβR1 stimulation or whether Cbfβ2 plays a direct role in maintaining their expression. Nevertheless, during the postnatal period, the expression of *Vdr* and *Bmpr1a* was higher in $Cbfb^{2m/2m}$ cells than in $Cbfb^{+/+}$ cells, indicating that Cbfβ2 is dispensable for the induction of these genes.

Results of this study and those of previous studies have established different roles for distinct members of the TGFβR superfamily in establishing and maintaining the primary LC network (Collin and Milne, 2016), inducing LC differentiation, and maintaining LC-lineage cells in a quiescent state. Regarding the physiological relevance of two TGFβ superfamily regulatory pathways, our results showed that loss of selective signaling that is involved in LC differentiation allows LC precursors to reside in the epidermis of $Cbfb^{2m/2m}$ mice; however, these cells lose developmental potential with time. It is unclear whether changes in developmental potency are a common feature of embryonic LC precursors that reside in the epidermis beyond the postnatal period, because no other models showing the retention of such cells have been reported. Thus, the exact mechanisms resulting in diminished developmental potential remain elusive. However, it is conceivable that LC precursors that cannot differentiate into LCs are useless and therefore should be eliminated from the epidermis. In this regard, two pathways composed of different TGFβR superfamily members might function to survey responsiveness to the TGFβ superfamily. A pathway that mediates the epidermal egress of undifferentiated LC precursors, which could result from either insufficient levels of BMP7/TGFβ1 in the skin environment or intrinsic defects in integrating those environmental cues, might be beneficial to vacate the space needed for the recruitment of BM-derived monocytes to restore the functional LC network. Thus, surveying the responsiveness to the TGFβ superfamily might increase a probability for meditating replenishment of the LC network by other resources. Given that LC differentiation from BM precursors was shown to be independent of TGFβR signaling (Borkowski et al., 1997), which is consistent with emergence of LC cells in older $Cbfb^{2m/2m}$ mice, the second adult LC developmental program would restore the LC network even after the primary LC network fails to differentiate from embryonic LC precursors. This hypothesis might explain why undifferentiated LC precursors are hardly detected in the adult epidermis. Contrary to TGFβR-independent LC differentiation from BM precursors in vivo, LC differentiation from BM cells in vitro depends on TGFβ/BMPR1A signaling. It is important to understand how BMPR1A signaling supports LC differentiation from BM cells in vitro.

Altogether, our results revealed an essential role for Cbfβ2 in the establishment of the primary LC network. Two major immune cell types, DETCs and LCs, are absent from the epidermis of Runx3- and Cbfβ2-deficient mice. Our comparative genomics approach showed that the splicing event that generates Cbfβ2 likely emerged as early as in bony fish (M. Tenno and I. Taniuchi, unpublished data), despite *Runx3* being already present in lamprey (Nah et al., 2014). A recent study showed that LC-like cells are present in catfish (Kordon et al., 2016), prompting us to speculate on an evolutionarily conserved role for Cbfβ2 in LC differentiation. Interestingly, the interaction between Runx2 and VDR was proposed to be involved in shaping the genetic program of osteoblastogenesis (Marcellini et al., 2010). Further understanding of the Cbfβ2-dependent establishment of LC networks in several species will improve understanding of the evolution of the skin immune system.

MATERIALS AND METHODS

Mice and study design

In order to generate the $Cbfb^{1m}$ and $Cbfb^{2m}$ mutant allele, the splicing donor signal in exon 5 of murine *Cbfb* gene was mutated by homologous recombination in embryonic stem cells. To generate the $Rosa26^{Cbfb2}$ allele, cDNA encoding Cbfβ2 was amplified by PCR to add AscI sites at both ends, and this was ligated into an AscI-cleaved pCTV vector (15912l Addgene). C57/BL6 mice congenic for the CD45 locus were purchased from Sankyo Labo Service Coro. CSF IR-iCre transgenic mice (JR019098) and $Rosa26^{ERT2Cre}$ mice were purchased from the Jackson Laboratory and Artemis Pharmaceuticals, respectively. $Cx3cr1^{gfp}$ reporter mice, $Rosa26^{YFP}$ reporter mice, and *CD11c-Cre* transgenic mice were a gift from S. Jung (Weizmann Institute of Science, Rehovot, Israel), F. Costantino (Columbia University, New York, NY), and B. Reizis (Columbia University), respectively. All animal experiments were performed in the animal facility at the RIK EN Center for Integrative Medical Sciences according to Institutional Animal Care Guidelines. Mice of different groups were cohoused and randomly assigned for analyses.

Cell preparation and flow cytometry analyses

To prepare single-cell suspensions from epidermis, ears were split into dorsal and ventral halves. After removal of cartilage, ears were incubated with 0.5% trypsin and 1 mM EDTA for 1 h at 37°C. The epidermis was peeled from the dermis and was dissociated into single cells by mashing through a 70-μm cell strainer (BD Biosciences). The resulting single-cell suspensions were stained with the following antibodies purchased from BD Biosciences or eBiosciences: CD4 (RM4-5), CD8 (53-6.7), B220 (RA3-6B2), CD11b (M1/70), CD45 (30-F11), CD45.1 (A20), CD45.2 (104), CD3 (145-2C11), MHC-II (M5/114.15.2), CD207 (eBioL31), CD11c (HL3), EpCAM (G8.8), CD24 (M1/69), F4/80 (BM8), CCR7 (4B12), and CD86 (GL1). For intracellular staining, cells were permeabilized before staining with antibodies. Multicolor flow cytometry analysis was performed using a BD FACScanto II (BD Biosciences), and data were analyzed using FlowJo (Tree Star) software. Cell subsets were sorted using a FACSAria II (BD Biosciences).

Preparation of epidermal sheet for immunohistochemistry

Ears were split into dorsal and ventral halves. After removal of cartilage and incubation in PBS containing 20 mM EDTA for 1 h at 37°C, the epidermis was peeled from dermis and fixed with 2% PFA in PBS for 30 min on ice. Fixed epidermal sheets were sequentially incubated with PBS, 25% MtOH/PBS, 50% MtOH/PBS, 75% MtOH/PBS, and 100% MtOH for 15 min on ice at each incubation. The epidermis was incubated with 100% MtOH at −20°C overnight. The next day, the epidermis was sequentially incubated with 100% MtOH, 75% MtOH/PBS, 50% MtOH/PBS, 25% MtOH/PBS, and PBS for 15 min on ice at each incubation. The epidermis was first blocked with 5% skim milk, 2% BSA, and 0.1% Triton X-100 in PBS for 1 h on ice then stained with anti-CD3, anti–MHC-II, anti-EpCAM, and anti-Langerin antibodies in blocking solution for 2 h, followed by five washes with PBS/0.05% Tween on ice. After being mounted on MAS-coated slides (Matsunami Glass) using Fluoromount (Diagnostic BioSystems), the stained epidermis sheet was analyzed using TCS SP2 AOBS fluorescent microscopy (Leica).

Real-time quantitative PCR

RNAs were isolated using TRIzol (Thermo Fisher Scientific) according to the manufacturer's instruction. cDNAs were synthesized from total RNAs with oligo dT primers using Superscript III reverse transcription (Invitrogen). Amplification was performed with SYBR Green Real-Time PCR Master Mix (Thermo Fisher Scientific). Primer sequences are listed in Table S1.

Parabiosis

Surgical procedures to generate parabiotic pairs between CD45.2 *Cbfb*$^{+/+}$ or *Cbfb*$^{2m/2m}$ and CD45.1 *Cbfb*$^{+/+}$ mice were performed as described previously (Rossi et al., 2005). After 7 mo, tissues of each mouse were dissected and analyzed by flow cytometry.

BM chimeras

Total BM cells (5×10^5 cells) from 8-wk-old CD45.1 *Cbfb*$^{+/+}$ mice were intravenously injected into sublethally irradiated (9.5 Gy) 6-wk-old CD45.2 *Cbfb*$^{+/+}$ or *Cbfb*$^{2m/2m}$ mice. 7 mo after injection, mice were killed, and flow cytometry analysis was performed.

Marking of yolk sac–derived cells by fate mapping. The marking of yolk sac–derived cells using *Rosa26*^{YFP} and *CSF1R-iCre* transgenic mouse strains was performed as previously described (Schulz et al., 2012). In brief, 4-OHT (2 mg/mouse; Sigma-Aldrich) and progesterone (4 mg/mouse; Sigma-Aldrich) were injected once at 8.5 dpc intraperitoneally into pregnant *Cbfb*$^{+/2m}$:*Rosa26*$^{+/YFP}$:*CSF1R-iCre* females, which were crossed with *Cbfb*$^{+/2m}$:*Rosa26*$^{+/YFP}$:*CSF1R-iCre* transgenic male mice. Epidermal tissues were prepared for flow cytometric analyses from offspring harboring the *Cbfb*$^{+/+}$:*Rosa26*$^{+/YFP}$:*CSF1R-iCre* or *Cbfb*$^{2m/2m}$:*Rosa26*$^{+/YFP}$:*CSF1R-iCre* genotype at 4 mo of age.

Conditional induction of Cbfβ2 from the *Rosa26*^{Cbfb2} allele. To induce *Cbfβ2* expression from the *Rosa26*^{Cbfb2} allele in *Cbfb*$^{2m/2m}$ mice at different ages, we first set up intercrossing between *Cbfb*$^{+/2m}$:*Rosa26*$^{Cbfb2/ERT2}$ mice. Topical administration of 4-OHT (1 mg/ml in EtOH) on the ears of all newborn pups was initiated at P0 and applied for an additional 4 d. Genotyping was performed at 1 wk of age, and pups harboring *Cbfb*$^{2m/2m}$:*Rosa26*$^{Cbfb2/ERT2}$ were selected for further analyses at 2 wks of age. *Cbfb*$^{2m/2m}$:*Rosa26*$^{Cbfb2/ERT2}$ mice at 4 wks of age were treated similarly, receiving topical administration of 4-OHT on the ears for 5 d; animals were analyzed 2 wks after the first 4-OHT treatment.

Digital RNA-seq and data analyses

100 CD45$^+$CD3$^-$MHC-II$^+$ cells were sorted from epidermis of P5 and 1.5-mo-old *Cbfb*$^{+/+}$ and *Cbfb*$^{2m/2m}$ mice into a tube using a FACSAria III (BD Biosciences). To normalize results using detection efficiency, the same amount of spike-in RNAs (a known number of External RNA Controls Consortium RNA molecules) was added into every tube, and the cells were lysed. After fragmentation of RNA molecules by temperature elevation, cDNAs were synthesized by reverse transcription using a reverse transcription primer in which the first common primer sequence molecular barcode, 14 T bases, and 1 V (A or G or C) base were tandemly arranged from the 5′ end. A second common primer sequence was also attached to the 3′ end of each generated cDNA molecule by template switching during reverse transcription. Subsequently, cDNAs were amplified using the primer that contains an Illumina adapter sequence, sample index, and the first common primer sequence with the other primer that contains another Illumina adapter sequence, sample index, and the second common primer sequence. Three independent libraries were generated from each subset with different sample indexes, and in total six libraries were sequenced together in

a single MiSeq run (150 cycles; Illumina). Sequencing data were mapped against the mouse genome (mm10 assembly) using TopHat2 (Kim et al., 2013). This strategy, called digital RNA-seq (Shiroguchi et al., 2012), provides the mean number of mRNA molecules per cell for each gene and each indexed sample by counting the number of unique molecular barcodes instead of the number of sequenced cDNA molecules. Differential gene expression of digital RNA-seq was determined using DESeq2. To identify genes differentially expressed among groups, a moderated one-way ANOVA was performed. Genes were considered differentially expressed when they had false discovery rates of <0.01 and log2 fold-changes of >1 or <−1. To evaluate the combinatorial gene expression changes of cytokine–receptor pairs, we first picked up all cytokines and receptors according to the annotations in UniProt database. Cytokine–receptor interactions were reconstructed based on the protein–protein interaction network in the STRING database. All sequencing datasets have been deposited in the Genome Expression Omnibus database under accession no. GSE95487.

In vitro culture for LCs
For the differentiation of LC-like cells from BM progenitors (Chopin et al., 2013), lineage (CD4, CD8, B220, MHC-II, CD11b, CD11c, NK1.1, Ter119, and Gr-1)-maker negative fractions were prepared from the BM cells of *Cbfb*$^{+/+}$ and *Cbfb*$^{2m/2m}$ mice using the MACS system (Miltenyi Biotec). Cells (5×10^5) were cultured in RPMI 1640 (Nacalai Tesque) supplemented with 10% FCS, 20 ng/ml GM-CSF (R&D Systems), and 10 ng/ml TGFβ1 (R&D Systems) for 3 d in a 24-well plate in the absence or presence of 5 µM dorsomorphin (041-3376; Wako Chemicals) or 5 µM SB431542 (Cay-13031; Cayman Chemical). For inhibition assays, BM progenitors were pretreated with dorsomorphin or SB431542 1 h before adding cytokines.

Online supplemental material
Fig. S1 shows increased *Cbfb1* and *Cbfb2* expression during LC differentiation. Fig. S2 shows conditional and skin-specific induction of *Cbfb2* expression from the *Rosa26*^{Cbfb2} allele. Fig. S3 shows a summary of the analysis of cytokine–receptor pairs and expression levels of selected genes. Table S1 shows sequence information for primers used for real-time quantitative PCR.

ACKNOWLEDGMENTS

We thank M. Ikegaya for genotyping, T. Ishikura for embryonic stem cell aggregation, and K. Fukuhara for help in performing digital RNA sequencing.

This work was supported by Japan Society for the Promotion of Science KAKENHI grants 14F04214 and JP 19390118 (I. Taniuchi) and JP 23790552 (M. Tenno), the RIKEN Center for Integrative Medical Sciences YCI program (K. Shiroguchi), and Japan Science and Technology Agency/PRESTO grant JPMJPR15F3 (K. Shiroguchi).

The authors declare no competing financial interests.

Author contributions: M. Tenno performed phenotypic analyses. K. Shiroguchi, E. Kawakami, K. Koseki, K. Kryukov, and T. Imanishi performed digital RNA-seq and analyzed data. S. Muroi generated mouse strains. F. Ginhoux provided essential advice to design experiments and helped to write the manuscript. I. Taniuchi designed experiments and wrote the manuscript.

Submitted: 21 April 2017

Revised: 18 June 2017

Accepted: 14 July 2017

REFERENCES

Bauer, T., A. Zagórska, J. Jurkin, N. Yasmin, R. Köffel, S. Richter, B. Gesslbauer, G. Lemke, and H. Strobl. 2012. Identification of Axl as a downstream effector of TGF-β1 during Langerhans cell differentiation and epidermal homeostasis. *J. Exp. Med.* 209:2033–2047. http://dx.doi.org/10.1084/jem.20120493

Bennett, C.L., E. van Rijn, S. Jung, K. Inaba, R.M. Steinman, M.L. Kapsenberg, and B.E. Clausen. 2005. Inducible ablation of mouse Langerhans cells diminishes but fails to abrogate contact hypersensitivity. *J. Cell Biol.* 169:569–576. http://dx.doi.org/10.1083/jcb.200501071

Bobr, A., B.Z. Igyarto, K.M. Haley, M.O. Li, R.A. Flavell, and D.H. Kaplan. 2012. Autocrine/paracrine TGF-β1 inhibits Langerhans cell migration. *Proc. Natl. Acad. Sci. USA.* 109:10492–10497. http://dx.doi.org/10.1073/pnas.1119178109

Borkowski, T.A., J.J. Letterio, A.G. Farr, and M.C. Udey. 1996. A role for endogenous transforming growth factor β 1 in Langerhans cell biology: The skin of transforming growth factor β 1 null mice is devoid of epidermal Langerhans cells. *J. Exp. Med.* 184:2417–2422. http://dx.doi.org/10.1084/jem.184.6.2417

Borkowski, T.A., J.J. Letterio, C.L. Mackall, A. Saitoh, X.J. Wang, D.R. Roop, R.E. Gress, and M.C. Udey. 1997. A role for TGFβ1 in langerhans cell biology. Further characterization of the epidermal Langerhans cell defect in TGFβ1 null mice. *J. Clin. Invest.* 100:575–581. http://dx.doi.org/10.1172/JCI119567

Chen, W., and P. Ten Dijke. 2016. Immunoregulation by members of the TGFβ superfamily. *Nat. Rev. Immunol.* 16:723–740. http://dx.doi.org/10.1038/nri.2016.112

Chopin, M., and S.L. Nutt. 2015. Establishing and maintaining the Langerhans cell network. *Semin. Cell Dev. Biol.* 41:23–29. http://dx.doi.org/10.1016/j.semcdb.2014.02.001

Chopin, M., C. Seillet, S. Chevrier, L. Wu, H. Wang, H.C. Morse III, G.T. Belz, and S.L. Nutt. 2013. Langerhans cells are generated by two distinct PU.1-dependent transcriptional networks. *J. Exp. Med.* 210:2967–2980. http://dx.doi.org/10.1084/jem.20130930

Chorro, L., A. Sarde, M. Li, K.J. Woollard, P. Chambon, B. Malissen, A. Kissenpfennig, J.B. Barbaroux, R. Groves, and F. Geissmann. 2009. Langerhans cell (LC) proliferation mediates neonatal development, homeostasis, and inflammation-associated expansion of the epidermal LC network. *J. Exp. Med.* 206:3089–3100. http://dx.doi.org/10.1084/jem.20091586

Collin, M., and P. Milne. 2016. Langerhans cell origin and regulation. *Curr. Opin. Hematol.* 23:28–35. http://dx.doi.org/10.1097/MOH.0000000000000202

Fainaru, O., E. Woolf, J. Lotem, M. Yarmus, O. Brenner, D. Goldenberg, V. Negreanu, Y. Bernstein, D. Levanon, S. Jung, and Y. Groner. 2004. Runx3 regulates mouse TGF-β-mediated dendritic cell function and its absence results in airway inflammation. *EMBO J.* 23:969–979. http://dx.doi.org/10.1038/sj.emboj.7600085

Gaiser, M.R., T. Lämmermann, X. Feng, B.Z. Igyarto, D.H. Kaplan, L. Tessarollo, R.N. Germain, and M.C. Udey. 2012. Cancer-associated epithelial cell adhesion molecule (EpCAM; CD326) enables epidermal Langerhans cell motility and migration in vivo. *Proc. Natl. Acad. Sci. USA.* 109:E889–E897. http://dx.doi.org/10.1073/pnas.1117674109

Ginhoux, F., and M. Merad. 2010. Ontogeny and homeostasis of Langerhans cells. *Immunol. Cell Biol.* 88:387–392. http://dx.doi.org/10.1038/icb.2010.38

Ginhoux, F., F. Tacke, V. Angeli, M. Bogunovic, M. Loubeau, X.M. Dai, E.R. Stanley, G.J. Randolph, and M. Merad. 2006. Langerhans cells arise from monocytes in vivo. *Nat. Immunol.* 7:265–273. http://dx.doi.org/10.1038/ni1307

Hieronymus, T., M. Zenke, J.H. Baek, and K. Seré. 2015. The clash of Langerhans cell homeostasis in skin: Should I stay or should I go? *Semin. Cell Dev. Biol.* 41:30–38. http://dx.doi.org/10.1016/j.semcdb.2014.02.009

Hoeffel, G., Y. Wang, M. Greter, P. See, P. Teo, B. Malleret, M. Leboeuf, D. Low, G. Oller, F. Almeida, et al. 2012. Adult Langerhans cells derive predominantly from embryonic fetal liver monocytes with a minor contribution of yolk sac-derived macrophages. *J. Exp. Med.* 209:1167–1181. http://dx.doi.org/10.1084/jem.20120340

Ito, Y., and K. Miyazono. 2003. RUNX transcription factors as key targets of TGF-β superfamily signaling. *Curr. Opin. Genet. Dev.* 13:43–47. http://dx.doi.org/10.1016/S0959-437X(03)00007-8

Kaplan, D.H., M.O. Li, M.C. Jenison, W.D. Shlomchik, R.A. Flavell, and M.J. Shlomchik. 2007. Autocrine/paracrine TGFβ1 is required for the development of epidermal Langerhans cells. *J. Exp. Med.* 204:2545–2552. http://dx.doi.org/10.1084/jem.20071401

Kel, J.M., M.J.H. Girard-Madoux, B. Reizis, and B.E. Clausen. 2010. TGF-β is required to maintain the pool of immature Langerhans cells in the epidermis. *J. Immunol.* 185:3248–3255. http://dx.doi.org/10.4049/jimmunol.1000981

Kim, D., G. Pertea, C. Trapnell, H. Pimentel, R. Kelley, and S.L. Salzberg. 2013. TopHat2: Accurate alignment of transcriptomes in the presence of insertions, deletions and gene fusions. *Genome Biol.* 14:R36. http://dx.doi.org/10.1186/gb-2013-14-4-r36

Kordon, A.O., M.A. Scott, I. Ibrahim, H. Abdelhamed, H. Ahmed, W. Baumgartner, A. Karsi, and L.M. Pinchuk. 2016. Identification of Langerhans-like cells in the immunocompetent tissues of channel catfish, *Ictalurus punctatus*. *Fish Shellfish Immunol.* 58:253–258. http://dx.doi.org/10.1016/j.fsi.2016.09.033

Li, G., X.H. Gao, and Q.S. Mi. 2016. TGF-β1-Smad signaling pathways are not required for epidermal LC homeostasis. *Oncotarget.* 7:15290–15291. http://dx.doi.org/10.18632/oncotarget.8167

Marcellini, S., C. Bruna, J.P. Henríquez, M. Albistur, A.E. Reyes, E.H. Barriga, B. Henríquez, and M. Montecino. 2010. Evolution of the interaction between Runx2 and VDR, two transcription factors involved in osteoblastogenesis. *BMC Evol. Biol.* 10:78. http://dx.doi.org/10.1186/1471-2148-10-78

Merad, M., M.G. Manz, H. Karsunky, A. Wagers, W. Peters, I. Charo, I.L. Weissman, J.G. Cyster, and E.G. Engleman. 2002. Langerhans cells renew in the skin throughout life under steady-state conditions. *Nat. Immunol.* 3:1135–1141. http://dx.doi.org/10.1038/ni852

Merad, M., F. Ginhoux, and M. Collin. 2008. Origin, homeostasis and function of Langerhans cells and other langerin-expressing dendritic cells. *Nat. Rev. Immunol.* 8:935–947. http://dx.doi.org/10.1038/nri2455

Mishina, Y., A. Suzuki, N. Ueno, and R.R. Behringer. 1995. Bmpr encodes a type I bone morphogenetic protein receptor that is essential for gastrulation during mouse embryogenesis. *Genes Dev.* 9:3027–3037. http://dx.doi.org/10.1101/gad.9.24.3027

Nagao, K., F. Ginhoux, W.W. Leitner, S. Motegi, C.L. Bennett, B.E. Clausen, M. Merad, and M.C. Udey. 2009. Murine epidermal Langerhans cells and langerin-expressing dermal dendritic cells are unrelated and exhibit distinct functions. *Proc. Natl. Acad. Sci. USA.* 106:3312–3317. http://dx.doi.org/10.1073/pnas.0807126106

Nah, G.S., B.H. Tay, S. Brenner, M. Osato, and B. Venkatesh. 2014. Characterization of the Runx gene family in a jawless vertebrate, the Japanese lamprey (*Lethenteron japonicum*). *PLoS One.* 9:e113445. http://dx.doi.org/10.1371/journal.pone.0113445

Ogawa, E., M. Inuzuka, M. Maruyama, M. Satake, M. Naito-Fujimoto, Y. Ito, and K. Shigesada. 1993. Molecular cloning and characterization of PEBP2 β, the heterodimeric partner of a novel *Drosophila* runt-related DNA binding protein PEBP2 α. *Virology.* 194:314–331. http://dx.doi.org/10.1006/viro.1993.1262

Perdiguero, E.G., and F. Geissmann. 2016. The development and maintenance of resident macrophages. *Nat. Immunol.* 17:2–8. http://dx.doi.org/10.1038/ni.3341

Romani, N., B.E. Clausen, and P. Stoitzner. 2010. Langerhans cells and more: Langerin-expressing dendritic cell subsets in the skin. *Immunol. Rev.* 234:120–141. http://dx.doi.org/10.1111/j.0105-2896.2009.00886.x

Rossi, F.M., S.Y. Corbel, J.S. Merzaban, D.A. Carlow, K. Gossens, J. Duenas, L. So, L. Yi, and H.J. Ziltener. 2005. Recruitment of adult thymic progenitors is regulated by P-selectin and its ligand PSGL-1. *Nat. Immunol.* 6:626–634. http://dx.doi.org/10.1038/ni1203

Schlitzer, A., V. Sivakamasundari, J. Chen, H.R. Sumatoh, J. Schreuder, J. Lum, B. Malleret, S. Zhang, A. Larbi, F. Zolezzi, et al. 2015. Identification of cDC1- and cDC2-committed DC progenitors reveals early lineage priming at the common DC progenitor stage in the bone marrow. *Nat. Immunol.* 16:718–728. http://dx.doi.org/10.1038/ni.3200

Schulz, C., E. Gomez Perdiguero, L. Chorro, H. Szabo-Rogers, N. Cagnard, K. Kierdorf, M. Prinz, B. Wu, S.E.W. Jacobsen, J.W. Pollard, et al. 2012. A lineage of myeloid cells independent of Myb and hematopoietic stem cells. *Science.* 336:86–90. http://dx.doi.org/10.1126/science.1219179

Seré, K., J.H. Baek, J. Ober-Blöbaum, G. Müller-Newen, F. Tacke, Y. Yokota, M. Zenke, and T. Hieronymus. 2012. Two distinct types of Langerhans cells populate the skin during steady state and inflammation. *Immunity.* 37:905–916. http://dx.doi.org/10.1016/j.immuni.2012.07.019

Shiroguchi, K., T.Z. Jia, P.A. Sims, and X.S. Xie. 2012. Digital RNA sequencing minimizes sequence-dependent bias and amplification noise with optimized single-molecule barcodes. *Proc. Natl. Acad. Sci. USA.* 109:1347–1352. http://dx.doi.org/10.1073/pnas.1118018109

Sparber, F., C.H. Tripp, K. Komenda, J.M. Scheffler, B.E. Clausen, L.A. Huber, N. Romani, and P. Stoitzner. 2015. The late endosomal adaptor molecule p14 (LAMTOR2) regulates TGFβ1-mediated homeostasis of Langerhans cells. *J. Invest. Dermatol.* 135:119–129. http://dx.doi.org/10.1038/jid.2014.324

Wang, Q., T. Stacy, J.D. Miller, A.F. Lewis, T.L. Gu, X. Huang, J.H. Bushweller, J.C. Bories, F.W. Alt, G. Ryan, et al. 1996. The CBFβ subunit is essential for CBFα2 (AML1) function in vivo. *Cell.* 87:697–708. http://dx.doi.org/10.1016/S0092-8674(00)81389-6

Xu, Y.P., Y. Shi, Z.Z. Cui, H.H. Jiang, L. Li, X.F. Wang, L. Zhou, and Q.S. Mi. 2012. TGFβ/Smad3 signal pathway is not required for epidermal Langerhans cell development. *J. Invest. Dermatol.* 132:2106–2109. http://dx.doi.org/10.1038/jid.2012.71

Yasmin, N., T. Bauer, M. Modak, K. Wagner, C. Schuster, R. Köffel, M. Seyerl, J. Stöckl, A. Elbe-Bürger, D. Graf, and H. Strobl. 2013a. Identification of bone morphogenetic protein 7 (BMP7) as an instructive factor for human epidermal Langerhans cell differentiation. *J. Exp. Med.* 210:2597–2610. http://dx.doi.org/10.1084/jem.20130275

Yasmin, N., S. Konradi, G. Eisenwort, Y.M. Schichl, M. Seyerl, T. Bauer, J. Stöckl, and H. Strobl. 2013b. β-Catenin promotes the differentiation of epidermal Langerhans dendritic cells. *J. Invest. Dermatol.* 133:1250–1259. http://dx.doi.org/10.1038/jid.2012.481

Zhang, X., J. Gu, F.S. Yu, L. Zhou, and Q.S. Mi. 2016. TGF-β1-induced transcription factor networks in Langerhans cell development and maintenance. *Allergy.* 71:758–764. http://dx.doi.org/10.1111/all.12871

Zouvelou, V., O. Passa, K. Segklia, S. Tsalavos, D.M. Valenzuela, A.N. Economides, and D. Graf. 2009. Generation and functional characterization of mice with a conditional BMP7 allele. *Int. J. Dev. Biol.* 53:597–603. http://dx.doi.org/10.1387/ijdb.082648vz